

Role of element-specific damping on the ultrafast, helicity-independent all-optical switching dynamics in amorphous (Gd,Tb)Co thin films.

Alejandro Ceballos,^{1,2,*} Akshay Pattabi,^{3,*} Amal El-Ghazaly,³ Sergiu Ruta,⁴ Christian P Simon,⁵ Richard F L Evans,⁴ Thomas Ostler,^{6,7} Roy W Chantrell,⁴ Ellis Kennedy,^{1,8} Mary Scott,^{1,8} Jeffrey Bokor,^{3,2} and Frances Hellman^{1,2,5}

¹Department of Materials Science and Engineering, University of California Berkeley, Berkeley, California 94720, USA

²Materials Sciences Division, Lawrence Berkeley National Laboratory, Berkeley, California 94720, USA

³Department of Electrical Engineering and Computer Sciences, University of California, Berkeley, Berkeley, CA 94720, USA

⁴Department of Physics, University of York, Heslington, York YO10 5DD, United Kingdom

⁵Department of Physics, University of California, Berkeley, Berkeley, California 94720, USA

⁶Materials and Engineering Research Institute, Sheffield Hallam University, Howard Street, Sheffield S1 1WB, UK

⁷Faculty of Science, Technology and Arts, Sheffield Hallam University, Howard Street, Sheffield, S1 1WB, UK

⁸National Center for Electron Microscopy, Molecular Foundry, Lawrence Berkeley National Laboratory, Berkeley, CA 94720

Ultrafast control of the magnetization in ps timescales by fs laser pulses offers an attractive avenue for applications such as fast magnetic devices for logic and memory. However, ultrafast helicity-independent all-optical switching (HI-AOS) of the magnetization has thus far only been observed in Gd-based, ferrimagnetic amorphous (*a*-) rare earth-transition metal (*a*-RE-TM) systems, and a comprehensive understanding of the reversal mechanism remains elusive. Here, we report HI-AOS in ferrimagnetic *a*-Gd_{22-x}Tb_xCo₇₈ thin films, from $x = 0$ to $x = 18$, and elucidate the role of Gd in HI-AOS in *a*-RE-TM alloys and multilayers. Increasing Tb content results in increasing perpendicular magnetic anisotropy and coercivity, without modifying magnetization density, and slower remagnetization rates and higher critical fluences for switching but still shows picosecond HI-AOS. Simulations of the atomistic spin dynamics based on the two-temperature model reproduce these results qualitatively and predict that the lower damping on the RE sublattice arising from the small spin-orbit coupling of Gd (with $L = 0$) is instrumental for the faster dynamics and lower critical fluences of the Gd-rich alloys. Annealing *a*-Gd₁₀Tb₁₂Co₇₈ leads to slower dynamics which we argue is due to an increase in damping. These simulations strongly indicate that accounting for element-specific damping is crucial in understanding HI-AOS phenomena. The results suggest that engineering the element specific damping of materials can open up new classes of materials that exhibit low-energy, ultrafast HI-AOS.

I. INTRODUCTION

The ability to control magnetism at short ps and sub-ps timescales has tantalized scientists since the discovery in 1996 of the ultrafast demagnetization of Ni following irradiation by fs laser pulses,[1] opening up the field of ultrafast magnetization dynamics. A major breakthrough was the discovery of helicity-independent all-optical switching (HI-AOS) of the magnetization, sometimes referred to as thermally-induced magnetization switching (TIMS), in ferrimagnetic *a*-Gd-Fe-Co alloys[2–4] in ps timescales by a single fs laser pulse. This magnetization switching phenomenon is unique in the field of all-optical switching as it exhibits one of the fastest switching speeds recorded[5], it is reversible and cyclable for 1000s of repetitions, and it is thermally-driven by a single laser pulse irrespective of polarization, i.e. no transfer of angular momentum from the laser is involved. HI-AOS offers the possibility of promising technological applications in high-speed, energy-efficient and non-volatile magnetic memory and logic, with two to three orders of magnitude higher operating speeds compared to conventional spintronic devices that operate on mechanisms such as external field control,[6] spin-transfer-torque,[7, 8] or spin-orbit torque.[9]

Despite significant advances in the field, a complete understanding of the mechanism of HI-AOS still remains lacking. Thus far, deterministic ultrafast toggle switching of the magnetization by a single laser pulse – where the switched area is controlled just by local heating from the spatial distribution of the laser pulse fluence – is predominantly found in Gd-based *a*-RE-TM ferrimagnetic alloys and multilayers. These include *a*-Gd-Fe-Co,[2–4] *a*-Gd-Co,[10] Pt/Co/Gd,[11] and exchange coupled Co/Pt/Co/*a*-GdFeCo[12] systems. Similar Tb-based ferrimagnetic systems such as *a*-Tb-Co alloys[13] have so far only shown helicity-dependent AOS (HD-AOS), requiring multiple circularly polarized laser pulses over longer timescales (μ s to ms), [14] or transient reversal with a single laser pulse, [15] wherein the magnetization reverts back to its original direction after a short reversal of a few ps. However, single-shot HI-AOS was demonstrated in Tb/Co multilayers when the layer thickness ratio of Co and Tb was within 1.3 - 1.5,[16] although the switching dynamics were not reported. HI-AOS was also demonstrated in an *a*-Tb₂₂Fe₆₉Co₉ alloy,[17] but required patterning of nanoscale antennas to enhance the optical field, thereby confining the switched region to less than 100 nm in areas near and around the antennas. The switching in that experiment was strongly influenced by inhomogeneities and control of the uniformity in the switched area under the laser pulse fluence profile could not be achieved.

* These two authors contributed equally

A complete microscopic theory has yet to explain the intrinsic fundamental physics of HI-AOS. In this work the role of

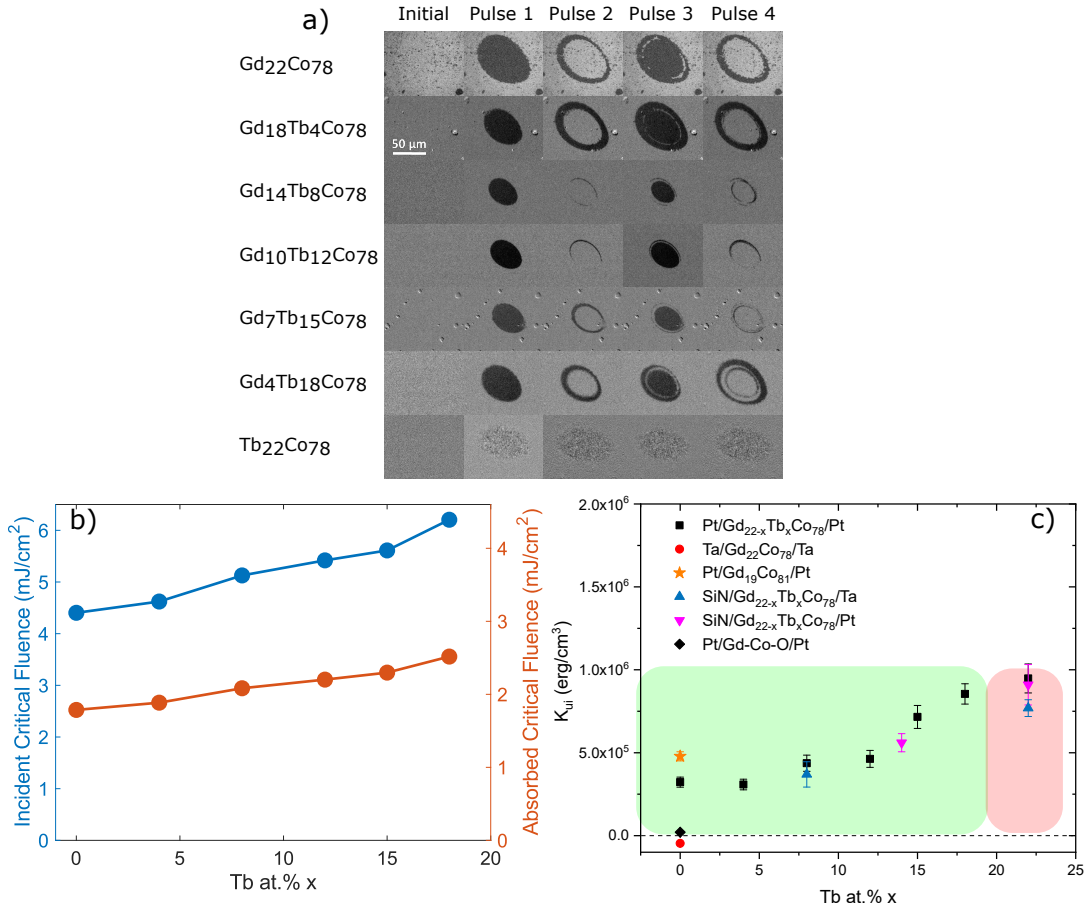


FIG. 1. a) MOKE microscopy images of Ta(3nm)/Pt(3)/*a*-Gd_{22-x}Tb_xCo₇₈(10)/Pt(3) thin films following a series of single laser pulses at an incident fluence of 6.9 mJ/cm², illustrate samples' ability to all-optically reverse their magnetization upon irradiation. Samples with a Tb concentration of up to 18 at.% exhibited HI-AOS while *a*-Tb₂₂Co₇₈ only exhibited demagnetization as evidenced by the nucleation of random domains. b) Incident and absorbed critical fluence increase with increasing Tb content. c) Intrinsic anisotropy constant K_{ii} vs Tb atomic percent in *a*-Gd_{22-x}Tb_xCo₇₈ thin films with various capping and underlayers as shown in the legend. Anisotropy increases with increasing Tb content for fixed under and overlayers. Pt under or overlayers increased K_{ii} for fixed *x*. The green box shows the compositions that exhibited HI-AOS; the red box those that did not. The effect of growing on different substrates and capping layers was tested but it had no effect on HI-AOS. Four *a*-Gd-Co samples with varying Gd/Co ratio are shown at *x* = 0. At the top, indicated with an orange star, is *a*-Gd₁₉Co₈₁ with compensation *T* below RT exhibiting PMA and HI-AOS. Beneath it the black square *a*-Gd₂₂Co₇₈ which is part of the main study; it has Pt under and over layers and exhibits PMA and HI-AOS. The black diamond is Gd-Co-O also with Pt over and underlayers, but grown in a reactive oxygen atmosphere, with K_{ii} value of 2.05×10^4 erg/cm³ and M_S of 40 emu/cm³. It exhibited HI-AOS though its dynamics were not studied. In red is *a*-Gd₂₂Co₇₈ with Ta under and over layers; it has in-plane magnetization which cannot be probed using polar MOKE, hence it's unknown if it exhibits HI-AOS.

Gd in enabling HI-AOS was investigated experimentally and theoretically by studying *a*-Gd_{22-x}Tb_xCo₇₈ thin films. Vapor deposited *a*-RE-TM films have long been known to possess significant perpendicular magnetic anisotropy (PMA) leading them to have been considered and sometimes used as magnetic recording media for decades. PMA is intrinsic to the structure, a result of subtle structural ordering due to growth processes[18, 19]. Tb has significant orbital angular momentum compared to Gd ($L = 3$ compared to $L = 0$) and greater spin-orbit coupling than Gd, leading to the large PMA and larger magnetic damping[20, 21]. By systematically replacing the Gd atoms with Tb atoms (such that the RE composition is kept constant), and by post-growth annealing, the anisotropy, magnetic damping and spin-orbit coupling (SOC) are modi-

fied, while the magnetization and the Curie and compensation temperatures are held constant.

HI-AOS was found in *a*-Gd_{22-x}Tb_xCo₇₈ films up to *x* = 18, while *a*-Tb₂₂Co₇₈ only demagnetized upon laser irradiation. The threshold or critical fluence of the pulse needed for switching increased linearly with increasing Tb concentration and the switching dynamics became slower, indicating increasing difficulties in the switching process with increasing Tb. Annealing *a*-Gd₁₀Tb₁₂Co₇₈ (a high *x* hence high magnetic anisotropy film) at 300 °C for one hour reduced the anisotropy by an order of magnitude (without changing the magnetization), due to increased randomization of the local uniaxial anisotropy fields that lead to PMA. This then increases the damping and is here shown to yield slower re-

magnetization dynamics but no change in critical fluence. These slower dynamics with no change in critical fluence are reproduced in simulations with increased damping. Simulations of the atomistic spin dynamics using the VAMPIRE software package[22, 23] combined with a two-temperature model (2TM)[4] indicate that these results can be explained by an increased damping on the RE site when Gd is replaced by Tb. The results and simulations suggest that engineering the relative element-specific damping of the RE and TM sublattices can be used to find new materials that exhibit HI-AOS. Increased anisotropy with Tb content, and decreased anisotropy by annealing both led to slower switching dynamics, indicating that anisotropy is not a significant factor in HI-AOS. The high perpendicular magnetic anisotropy in Tb-rich films make them attractive candidates for magnetic devices with higher memory storage densities and retention times that exploit the fast read-write speeds of HI-AOS.

II. RESULTS

A. Single-shot HI-AOS in *a*-GdTbCo alloys

Amorphous, ferrimagnetic thin-films of Ta(3)/Pt(3)/*a*-Gd_{22-x}Tb_xCo₇₈(10)/Pt(3) (thicknesses are in nm) heterostructures were sputter deposited onto substrates of Si(525μm)/SiO₂(50nm)/SiN_x(300 nm). The *a*-Gd-Tb-Co films were co-deposited from separate Tb, Gd and Co targets with Pt or Ta over and underlayers grown *in situ* (Methods section at the end). Energy dispersive spectroscopy images taken with a scanning transmission electron microscope found no evidence of inhomogeneities at the 10 nm scale as had been reported in previous work on *a*-Gd-Fe-Co[24] (See suppl. matls.). The magnetization was measured with a Quantum Design MPMS SQUID magnetometer as a function of field and temperature. Room temperature saturation M_s (~ 100 emu/cm³) and compensation temperature T_M (~ 400 K) were independent of x , due to the fixed 22 at.% RE content. The intrinsic perpendicular magnetic anisotropy constant K_{ui} increased with increasing x , from 4×10^5 ergs/cm³ for *a*-Gd₂₂Co₇₈ to 2×10^6 ergs/cm³ for *a*-Tb₂₂Co₇₈. At room temperature, the magnetization of all the films studied is RE-dominant. The Curie temperature of all films was found to be greater than 600 K.

The magnetization of the samples is initialized at room temperature with an external out of plane magnetic field of ~ 0.7 T, fully saturating all samples. The field is then turned off, and the samples are irradiated with 100 fs full-width half maximum (FWHM) optical pulses from a regeneratively amplified Ti-Sapphire laser. Magneto Optical Kerr Effect (MOKE) microscope images depict single shot switching of the magnetization of all films except *a*-Tb₂₂Co₇₈ as shown in Fig. 1a. Films with as much as 18 at.% Tb (and hence as little as 4 at.% Gd) have deterministic magnetization reversal upon irradiation with a single laser pulse. Amorphous Tb₂₂Co₇₈ only shows demagnetization, evidenced by the nucleation of random magnetic domains. Further growth and characterization details are available in supplemental materials.

Fig. 1b shows that increasing the Tb content increases the incident critical fluence, starting from 4.4 mJ/cm² for *a*-Gd₂₂Co₇₈ and linearly increasing to 6.2 mJ/cm² for *a*-Gd₄Tb₁₈Co₇₈. The absorbed critical fluence calculated from ellipsometry measurements of the optical properties of the films (see suppl. matls.) increases linearly from 1.8 mJ/cm² to 2.5 mJ/cm² for *a*-Gd₂₂Co₇₈ and *a*-Gd₄Tb₁₈Co₇₈ respectively.

The intrinsic anisotropy constant (K_{ui}) was measured at room temperature and is plotted as a function of Tb at.% in Fig. 1c. The anisotropy constant increases systematically with increased Tb due to its large single ion anisotropy. The effect of growing on Ta or SiN, and of capping with Ta or Pt are also shown in Fig. 1c; these over and under layers, particularly Pt, increase the magnetic anisotropy of these thin films, nearly certainly due to interfacial anisotropy effects of these high SOC elements. The HI-AOS was unaffected by these buffer layers, clear evidence that K_{ui} alone is not the relevant driving parameter for HI-AOS. We also note that several films of other RE/TM ratio were tested, with varying magnetization values M , including TM-dominant (low RE/TM ratio). These also exhibited HI-AOS, demonstrating that at least over a limited range of M , M is not a determining factor for the ability to show HI-AOS.

For $x = 0$, i.e. *a*-Gd-Co, a number of different types of films were prepared and measured, with different Gd/Co ratios and different K_{ui} , as shown in the legend and data of Fig 1c. With Pt over and underlayer, *a*-Gd-Co has PMA and shows HI-AOS. With Ta over and underlayer, *a*-Gd-Co has in plane anisotropy and polar MOKE cannot measure HI-AOS. A Gd-Co-O sample (black diamond in Fig. 1c) was grown via oxygen reactive sputtering and exhibited both PMA and HI-AOS, as well as a distinct blue hue compared to the metallic gray of all other samples. The origin of PMA in *a*-Gd-Co is still an open question[25], although this reactively-grown sample suggests that oxidation plays a significant role, and we have found that *a*-Gd-Co grown under very clean conditions and without Pt over or underlayers are magnetized in-plane, while slightly worse background pressure or deliberate O introduction yields PMA. Rutherford backscattering spectrometry (RBS) measurements of *a*-Gd₂₂Co₇₈ of the main study do not reveal an oxygen peak, but its presence is likely hidden by the overlap of the Si signal from the substrate. Simulations with SIMNRA[26] indicate that if oxygen is present in *a*-Gd₂₂Co₇₈ it is at most 5 at.% O. Therefore it's likely that the PMA in *a*-Gd-Co studied here is a combination of slight gettering of residual oxygen in the chamber, plus an interfacial contribution from heavy metal layers.

B. Time dynamics of HI-AOS of *a*-GdTbCo alloys

The temporal dynamics of the magnetization of the *a*-Gd_{22-x}Tb_xCo₇₈ films as they undergo HI-AOS was measured by time-resolved magneto optical Kerr effect (TR-MOKE) (see suppl. matls.). An incident fluence of 6.9 mJ/cm² was chosen for all TR-MOKE experiments as it slightly exceeds the incident critical fluence of *a*-Gd₄Tb₁₈Co₇₈, the sample with the highest critical fluence that was able to be switched.

Note that the dynamics are not affected by the fluence as shown in supplemental materials. Fig. 2a shows the ultra-fast magnetization dynamics of all samples. The magnetization reversal process follows a two-step behavior. In the first step a rapid initial drop in the magnetization occurs in which all films share a similar demagnetization process within the first picosecond post irradiation from the pump pulse. The second stage consists of remagnetization in the opposite direction as the system cools down, except for a -Tb₂₂Co₇₈. a -Gd₂₂Co₇₈ exhibits the fastest remagnetization time; with increasing Tb concentration, the remagnetization systematically slows. The remagnetization rate plateaus with 15% and 18% Tb samples exhibiting similar dynamics. Finally, a -Tb₂₂Co₇₈ only demagnetizes upon irradiation and then recovers its magnetization along its initial direction upon cooling. It is possible that a -Tb₂₂Co₇₈ exhibits a transient switching in the first few ps following irradiation, similar to the behavior reported by Alebrand et al.,[15] and modeled by Moreno et al.,[27], suggesting that switching could occur at a higher fluence. However, utilizing higher fluences led to irreversible damage of the sample as the laser ablated or burned the sample surface. By 200 ps all samples had remagnetized to about 80% of the saturation value as shown in supplemental materials.

Fig. 2b is a close up of the experimental data of Fig. 2a, and shows, after the initial fast demagnetization step, behavior that deviates from exponential decay functions that appears to be more linear in character. The duration of this more linear behavior increases with increasing Tb before resuming exponential decay characteristics.

C. Simulation of HI-AOS in a -GdTbCo alloys

Atomistic spin dynamics simulations using the VAMPIRE software package[22, 23] combined with a two-temperature model (2TM)[4] (details discussed in suppl. mats.) were performed to simulate the experimental magnetization dynamics. These simulations incorporate the Hamiltonian of the system, which includes the exchange and anisotropy energies of Gd, Tb and Co, into the Landau-Lifshitz-Gilbert equation to compute the dynamics. As shown in Fig. 2c the simulations are in excellent agreement with the experiments, reproducing the characteristic behavior of similar demagnetization dynamics followed by increasingly slow remagnetization times with increasing Tb content. The bump in the magnetization following the initial demagnetization step is clearly seen in simulation, and exhibits a more linear character with increasing Tb as seen experimentally. The approximately factor of two discrepancy in the time scales between experiment and simulation is due to both the small size of the simulated system, which does not allow for domain dynamics to be taken in consideration, and also due to heat dissipation effects.

The simulations were only able to reproduce the experimental data when the element specific damping of the Gd, Tb and Co sites were assigned separately, rather than when using a net damping of the system as is typically done when simulating such RE-TM systems [27–29] (see suppl. mats. for comparison). This is consistent with previous experimen-

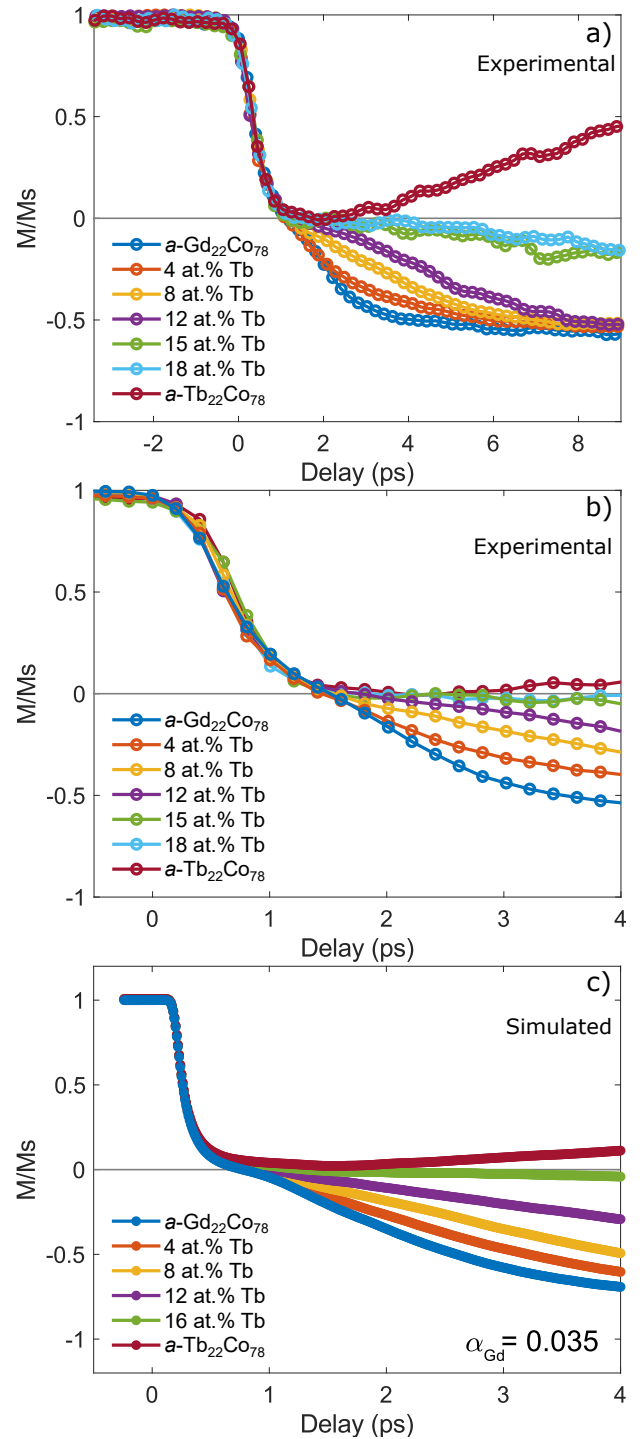


FIG. 2. a) Time-resolved magnetization dynamics of a -Gd_{22-x}Tb_xCo₇₈ thin films following irradiation with laser pulses of 6.9 mJ/cm² fluence and 100 fs pulsewidth. The initial rapid drop in magnetization is similar across all samples, but upon entering the remagnetization regime different rates are observed. b) Close up of the experimental data showing a bump in the magnetization (at ~ 1 ps) following the initial demagnetization step. c) Simulation results of the magnetization dynamics of Gd_{22-x}Tb_xCo₇₈ after laser irradiation obtained with a two-temperature model neglecting spin-lattice coupling as described in the text. In this simulation, the damping coefficients for Tb and Co were 0.05[27] and the damping of Gd α_{Gd} was fixed at 0.035.

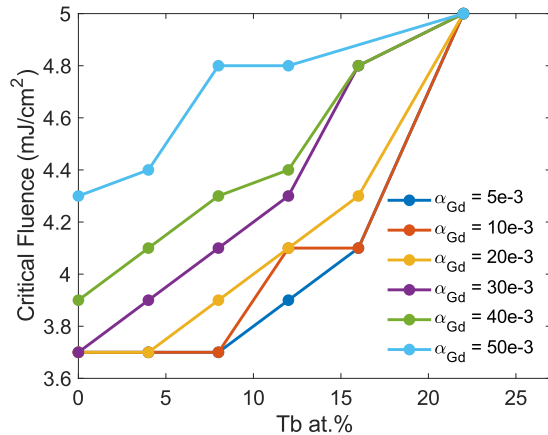


FIG. 3. Simulated critical fluence of a -Gd $_{22-x}$ Tb $_x$ Co $_{78}$ films as a function of Tb at.% x for different damping values of Gd, α_{Gd} . The Tb and Co damping parameters are constant (0.05). The critical fluence increases as α_{Gd} increases, indicating that lowering α_{Gd} reduces the threshold switching condition of a -Gd-Tb-Co alloys below the laser ablation limit.

tal and theoretical work on the role of damping in systems doped with RE[21, 30]. The experimental work of Radu et al. [21] on permalloy doped with RE showed increased damping for doping with Tb but no significant increase when doping with Gd. Ellis et al. [30] showed that element-specific damping is required to reproduce the macroscopic damping in such systems. In this work we varied the Gd/Tb ratio, as in the experiments, and fixed the element-specific damping value at 0.05 of the Tb and Co sites as in ref. [27]. The damping of Gd was taken to be lower than Tb and was varied between 0.005 and 0.05 in order to study its effect on the dynamics. In Fig. 2c, it is set at 0.035.

Fig. 3 shows the simulation results of critical fluence as a function of Tb concentration and varying Gd damping. The critical fluence for switching in the simulation is determined by the transition from non-deterministic to deterministic thermally induced switching. It shows that increasing the Tb content increases the critical fluence as observed experimentally, for all values of Gd damping. It also shows, that for a given concentration, increasing the damping on the Gd site increases the critical fluence.

D. Effect of annealing on switching dynamics

Annealing was used to test the influence of anisotropy and damping on the dynamics; the results are shown in Fig. 4. Annealing a -Gd $_{10}$ Tb $_{12}$ Co $_{78}$ at 300 °C for one hour results in a significant reduction in coercivity H_c and anisotropy K_{ui} (from 4.6×10^5 erg/cm 3 to 2.5×10^5 erg/cm 3) while maintaining the composition and M_S constant as seen in Fig 4b. Further annealing at 350 °C eliminated the PMA. The fact that M_S was unchanged by annealing strongly indicates that inhomogeneities such as phase segregation or crystallization have not occurred. The annealed sample shows a significantly slower re-

magnetization time, as seen in Fig. 4b. Atomistic simulations of the magnetization dynamics of this sample as a function of Gd damping are shown in Fig. 4c, which shows that increased damping increases the remagnetization time. It can be seen that increasing the damping on the Gd sites explains the slower remagnetization time, suggesting that the experimentally annealed sample has increased damping, in addition to reduced anisotropy. Work from Malinowski[31] et al. showed that introducing local variations of the anisotropy in amorphous CoFeB leads to an increase in the damping parameter. Since the origin of anisotropy in RE-TM alloys is due to a combination of pair-ordering and Tb's single ion anisotropy[18, 19], annealing of a -RE-TM alloys leads to a structural relaxation of pair-ordering that introduces local anisotropy variations. This in turn leads to higher damping and the slower remagnetization time observed. Fig. 2 showed that the samples with higher anisotropy (larger Tb at.%) show slower switching dynamics in both experiments and simulation. But the annealing study in Fig. 4 shows that the film with lower anisotropy exhibits slower switching. These observations lead us to conclude that it is the damping of the system, and not the anisotropy, that is the significant contributor to the ability to exhibit HI-AOS, consistent with the observation made in connection with Fig. 1 that HI-AOS was not determined by the magnitude of K_{ui} . Simulations shown in Fig. 4c with varying damping support this conclusion.

III. DISCUSSION

The experimental results show increasing critical fluence and remagnetization times with increasing Tb content, while post-growth annealing slowed the remagnetization rates. The simulations strongly indicate that the relative element specific damping of the rare earth site compared to the cobalt site is the key factor that influences the critical fluence required switching and the speed of remagnetization. As verified in the model for the annealed sample, at a fixed composition the key parameter that leads to slower remagnetization is the increased elemental damping. In simulation the damping constant is a phenomenological parameter that combines a host of diverse effects. Increasing the Tb composition leads to a greater spin-orbit interaction in the system, which is considered the intrinsic source of damping[32] and is proportional to ξ^2/W , where ξ is the spin orbital coupling energy and W is the d-band width[33]. Thus as the system becomes Tb-rich it experiences increased spin-orbit coupling which increases damping and thus leads to the dynamics observed in Fig. 2. For the dynamics observed in the annealed sample, the local spin-orbit coupling is very unlikely to have changed, but the anisotropy changed due to the structural relaxation and consequent randomization of local anisotropy axes induced by annealing, thereby increasing the macroscopic damping. The simulation does not directly account for spin-orbit coupling, but it indirectly simulates the effects of stronger spin-orbit coupling via increases in the damping parameter. As mentioned before the deterministic switching is independent of the anisotropy and therefore the main contribution of spin-orbit

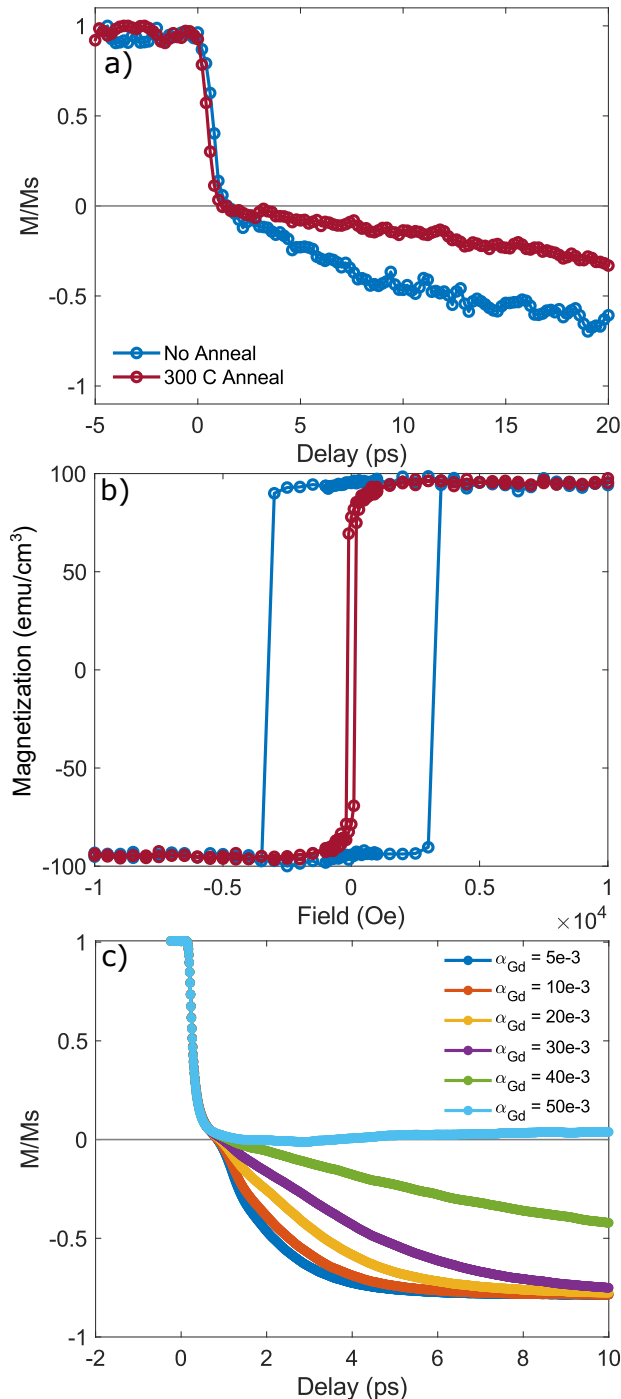


FIG. 4. a) Magnetization dynamics of $a\text{-Gd}_{10}\text{Tb}_{12}\text{Co}_{78}$ in the as-grown state (blue curve) and after annealing (red curve) at 300 °C for 1 hour. Annealing leads to a slower remagnetization time. b) Magnetization loops in the out-of-plane orientation show that annealing reduces the coercivity and anisotropy while M_S is unchanged. c) Simulated time-resolved magnetization dynamics of $a\text{-Gd}_{10}\text{Tb}_{12}\text{Co}_{78}$ as a function of increasing Gd damping. Increasing the damping leads to a slower remagnetization time, indicating that annealing leads to a higher damping value.

coupling for all optical switching is the damping. Therefore although the simulations reveal the critical role of damping in modifying the ultrafast magnetization dynamics, it is likely that the underlying physical mechanism is rooted in the spin-orbit interaction.

IV. CONCLUSION

In conclusion, we have shown that $a\text{-Gd}_{22-x}\text{Tb}_x\text{Co}_{78}$ thin films exhibit HI-AOS from $x = 0$ to $x = 18$, displaying a two-step reversal process with an identical fast demagnetization step and second slower remagnetization. The remagnetization time and the critical fluence increase as the Tb content increases, indicating that replacing Gd with Tb atoms hinders the switching process speed, but Tb helps increase PMA which is required for competitive memory storage technologies. Atomistic simulations explain the switching dynamics of our material system only after taking into account the individual element specific damping of each RE and TM sites. The slower remagnetization dynamics and the increased critical fluence as the Tb atomic percentage increases are explained on the basis of increased damping on the RE site upon addition of Tb. Annealing of an $a\text{-Gd}_{10}\text{Tb}_{12}\text{Co}_{78}$ film, which reduces K_{ui} and H_c without changing M , led to a slowing of the remagnetization rate without changing the critical fluence; these results are captured in simulations which indicate that reduced damping is responsible for modifying the ultrafast magnetization dynamics. The experimental inability to observe HI-AOS in $a\text{-TbCo}$ is due to the high critical fluence that under the present conditions is inaccessible without ablating the film. This suggests that better management of the laser thermal load may lead to HI-AOS beyond Gd-TM alloys. Our results indicate that the engineering of element specific damping of RE-TM systems will be crucial in endeavors to uncover material systems exhibiting HI-AOS with favorable properties (such as high anisotropy and large magnetization) for applications in ultrafast spintronic devices.

V. ACKNOWLEDGMENTS

This work was primarily supported by the Director, Office of Science, Office of Basic Energy Sciences, Materials Sciences and Engineering Division, of the U.S. Department of Energy under Contract No. DE-AC02-05-CH11231 within the Nonequilibrium Magnetic Materials Program (KC2204). Ultrafast laser measurements were supported by the NSF Center for Energy Efficient Electronics Science. A.C. acknowledges support by the National Science Foundation under Grant No. DGE 1106400. This project has received funding from the European Unions Horizon 2020 research and innovation programme under Grant Agreement No. 737093 (FEMTOTERABYTE). The atomistic simulations were undertaken on the VIKING cluster, which is a high performance compute facility provided by the University of York. We are grateful for computational support from the University of York High Performance Computing service, VIKING and the

Research Computing team.

A.C., A.P., A.E.-G., F.H., and J.B. conceived and planned the experiments. A.C. and C.S. grew and characterized the samples. Laser measurements were performed by A.P. and A.E.-G. Simulations were performed by S.R. on the

VAMPIRE software package developed by T.O., R.W.C. and R.F.L.E. TEM and EDS measurements were done by E.K. and M.S. A.C. and A.P. wrote the manuscript with input from all the authors.

-
- [1] E. Beaupaire, J.-C. Merle, A. Daunois, and J.-Y. Bigot, Ultrafast Spin Dynamics in Ferromagnetic Nickel, *Physical Review Letters* **76**, 4250 (1996).
- [2] C. D. Stanciu, A. Tsukamoto, A. V. Kimel, F. Hansteen, A. Kirilyuk, A. Itoh, and T. Rasing, Subpicosecond Magnetization Reversal across Ferrimagnetic Compensation Points, *Physical Review Letters* **99**, 10.1103/PhysRevLett.99.217204 (2007).
- [3] I. Radu, K. Vahaplar, C. Stamm, T. Kachel, N. Pontius, H. A. Drr, T. A. Ostler, J. Barker, R. F. L. Evans, R. W. Chantrell, A. Tsukamoto, A. Itoh, A. Kirilyuk, T. Rasing, and A. V. Kimel, Transient ferromagnetic-like state mediating ultrafast reversal of antiferromagnetically coupled spins, *Nature* **472**, 205 (2011).
- [4] T. Ostler, J. Barker, R. Evans, R. Chantrell, U. Atxitia, O. Chubykalo-Fesenko, S. El Moussaoui, L. Le Guyader, E. Mengotti, L. Heyderman, F. Nolting, A. Tsukamoto, A. Itoh, D. Afanasiev, B. Ivanov, A. Kalashnikova, K. Vahaplar, J. Mentink, A. Kirilyuk, T. Rasing, and A. Kimel, Ultrafast heating as a sufficient stimulus for magnetization reversal in a ferrimagnet, *Nature Communications* **3**, 10.1038/ncomms1666 (2012).
- [5] Y. Yang, R. B. Wilson, J. Gorchon, C.-H. Lambert, S. Salahuddin, and J. Bokor, Ultrafast magnetization reversal by picosecond electrical pulses, *Science Advances* **3**, 10.1126/sciadv.1603117 (2017), <https://advances.sciencemag.org/content/3/11/e1603117.full.pdf>
- [6] T. Gerrits, H. A. M. van den Berg, J. Hohlfield, L. Br, and T. Rasing, Ultrafast precessional magnetization reversal by picosecond magnetic field pulse shaping, *Nature* **418**, 10.1038/nature00905 (2002).
- [7] G. E. Rowlands, T. Rahman, J. A. Katine, J. Langer, A. Lyle, H. Zhao, J. G. Alzate, A. A. Kovalev, Y. Tserkovnyak, Z. M. Zeng, H. W. Jiang, K. Galatsis, Y. M. Huai, P. K. Amiri, K. L. Wang, I. N. Krivorotov, and J.-P. Wang, Deep subnanosecond spin torque switching in magnetic tunnel junctions with combined in-plane and perpendicular polarizers, *Applied Physics Letters* **98**, 102509 (2011), <https://doi.org/10.1063/1.3565162>.
- [8] H. Zhao, B. Glass, P. K. Amiri, A. Lyle, Y. Zhang, Y.-J. Chen, G. Rowlands, P. Upadhyaya, Z. Zeng, J. A. Katine, J. Langer, K. Galatsis, H. Jiang, K. L. Wang, I. N. Krivorotov, and J.-P. Wang, Sub-200 ps spin transfer torque switching in in-plane magnetic tunnel junctions with interface perpendicular anisotropy, *Journal of Physics D: Applied Physics* **45**, 025001 (2011).
- [9] K. Garello, C. O. Avci, I. M. Miron, M. Baumgartner, A. Ghosh, S. Auffret, O. Boulle, G. Gaudin, and P. Gambardella, Ultrafast magnetization switching by spin-orbit torques, *Applied Physics Letters* **105**, 212402 (2014), <https://doi.org/10.1063/1.4902443>.
- [10] A. El-Ghazaly, B. Tran, A. Ceballos, C.-H. Lambert, A. Patabi, S. Salahuddin, F. Hellman, and J. Bokor, Ultrafast magnetization switching in nanoscale magnetic dots, *Applied Physics Letters* **114**, 232407 (2019), <https://doi.org/10.1063/1.5098453>.
- [11] M. L. M. Lalieu, M. J. G. Peeters, S. R. R. Haenen, R. Lavrijsen, and B. Koopmans, Deterministic all-optical switching of synthetic ferrimagnets using single femtosecond laser pulses, *Physical Review B* **96**, 10.1103/PhysRevB.96.220411 (2017).
- [12] J. Gorchon, C.-H. Lambert, Y. Yang, A. Patabi, R. B. Wilson, S. Salahuddin, and J. Bokor, Single shot ultrafast all optical magnetization switching of ferromagnetic Co/Pt multilayers, *Applied Physics Letters* **111**, 042401 (2017).
- [13] S. Mangin, M. Gottwald, C.-H. Lambert, D. Steil, V. Uhl, L. Pang, M. Hehn, S. Alebrand, M. Cinchetti, G. Malinowski, Y. Fainman, M. Aeschlimann, and E. E. Fullerton, Engineered materials for all-optical helicity-dependent magnetic switching, *Nature Materials* **13**, 286 (2014).
- [14] M. S. El Hadri, P. Pirro, C.-H. Lambert, S. Petit-Watelot, Y. Quessab, M. Hehn, F. Montaigne, G. Malinowski, and S. Mangin, Two types of all-optical magnetization switching mechanisms using femtosecond laser pulses, *Phys. Rev. B* **94**, 064412 (2016).
- [15] S. Alebrand, U. Bierbrauer, M. Hehn, M. Gottwald, O. Schmitt, D. Steil, E. E. Fullerton, S. Mangin, M. Cinchetti, and M. Aeschlimann, Subpicosecond magnetization dynamics in TbCo alloys, *Physical Review B* **89**, 10.1103/PhysRevB.89.144404 (2014).
- [16] L. Avilés-Félix, L. Álvaro-Gómez, G. Li, C. Davies, A. Olivier, M. Rubio-Roy, S. Auffret, A. Kirilyuk, A. Kimel, T. Rasing, *et al.*, Integration of tb/co multilayers within optically switchable perpendicular magnetic tunnel junctions, *AIP Advances* **9**, 125328 (2019).
- [17] T.-M. Liu, T. Wang, A. H. Reid, M. Savoini, X. Wu, B. Koene, P. Granitzka, C. E. Graves, D. J. Higley, Z. Chen, G. Razinskas, M. Hantschmann, A. Scherz, J. Sthir, A. Tsukamoto, B. Hecht, A. V. Kimel, A. Kirilyuk, T. Rasing, and H. A. Drr, Nanoscale Confinement of All-Optical Magnetic Switching in TbFeCo - Competition with Nanoscale Heterogeneity, *Nano Letters* **15**, 6862 (2015).
- [18] V. G. Harris, K. D. Aylesworth, B. N. Das, W. T. Elam, and N. C. Koon, Structural origins of magnetic anisotropy in sputtered amorphous tb-fe films, *Phys. Rev. Lett.* **69**, 1939 (1992).
- [19] F. Hellman and E. Gyorgy, Growth-induced magnetic anisotropy in amorphous tb-fe, *Physical review letters* **68**, 1391 (1992).
- [20] S. E. Russek, P. Kabos, R. D. McMichael, C. Lee, W. E. Bailey, R. Ewasko, and S. C. Sanders, Magnetostriction and angular dependence of ferromagnetic resonance linewidth in tb-doped ni 0.8 fe 0.2 thin films, *Journal of applied physics* **91**, 8659 (2002).
- [21] I. Radu, G. Woltersdorf, M. Kiessling, A. Melnikov, U. Bovensiepen, J.-U. Thiele, and C. H. Back, Laser-induced magnetization dynamics of lanthanide-doped permalloy thin films, *Physical review letters* **102**, 117201 (2009).
- [22] R. F. L. Evans, W. J. Fan, P. Chureemart, T. A. Ostler, M. O. A. Ellis, and R. W. Chantrell, Atomistic spin model simulations of magnetic nanomaterials, *Journal of Physics Condensed Matter* **26**, 10.1088/0953-8984/26/10/103202 (2014).
- [23] VAMPIRE software package, Version 5. Available from <https://vampire.york.ac.uk/>.

- [24] C. E. Graves, A. H. Reid, T. Wang, B. Wu, S. de Jong, K. Vahaplar, I. Radu, D. P. Bernstein, M. Messerschmidt, L. Miller, R. Coffee, M. Bionta, S. W. Epp, R. Hartmann, N. Kimmel, G. Hauser, A. Hartmann, P. Holl, H. Gorke, J. H. Mentink, A. Tsukamoto, A. Fognini, J. J. Turner, W. F. Schlotter, D. Rolles, H. Soltau, L. Strder, Y. Acremann, A. V. Kimel, A. Kirilyuk, T. Rasing, J. Sth, A. O. Scherz, and H. A. Drr, Nanoscale spin reversal by non-local angular momentum transfer following ultrafast laser excitation in ferrimagnetic GdFeCo, *Nature Materials* **12**, 293 (2013).
- [25] N. Bergeard, A. Mougin, M. Izquierdo, E. Fonda, and F. Sirotti, Correlation between structure, electronic properties, and magnetism in $\text{Co}_x\text{Gd}_{1-x}$ thin amorphous films, *Phys. Rev. B* **96**, 064418 (2017).
- [26] M. Mayer, *SIMNRA user's guide* (Max-Planck-Institut für Plasmaphysik Garching, 1997).
- [27] R. Moreno, T. A. Ostler, R. W. Chantrell, and O. Chubykalo-Fesenko, Conditions for thermally induced all-optical switching in ferrimagnetic alloys: Modeling of TbCo, *Physical Review B* **96**, 10.1103/PhysRevB.96.014409 (2017).
- [28] E. Iacocca, T.-M. Liu, A. Reid, Z. Fu, S. Ruta, P. Granitzka, E. Jal, S. Bonetti, A. Gray, C. Graves, *et al.*, Spin-current-mediated rapid magnon localisation and coalescence after ultrafast optical pumping of ferrimagnetic alloys, *Nature communications* **10**, 1756 (2019).
- [29] X. Lu, X. Zou, D. Hinzke, T. Liu, Y. Wang, T. Cheng, J. Wu, T. A. Ostler, J. Cai, U. Nowak, *et al.*, Roles of heating and helicity in ultrafast all-optical magnetization switching in tbfeo, *Applied Physics Letters* **113**, 032405 (2018).
- [30] M. Ellis, T. Ostler, and R. Chantrell, Classical spin model of the relaxation dynamics of rare-earth doped permalloy, *Physical Review B* **86**, 174418 (2012).
- [31] G. Malinowski, K. C. Kuiper, R. Lavrijsen, H. J. M. Swagten, and B. Koopmans, Magnetization dynamics and Gilbert damping in ultrathin Co48fe32b20 films with out-of-plane anisotropy, *Applied Physics Letters* **94**, 102501 (2009).
- [32] M. C. Hickey and J. S. Moodera, Origin of Intrinsic Gilbert Damping, *Physical Review Letters* **102**, 10.1103/PhysRevLett.102.137601 (2009).
- [33] P. He, X. Ma, J. W. Zhang, H. B. Zhao, G. Lpke, Z. Shi, and S. M. Zhou, Quadratic Scaling of Intrinsic Gilbert Damping with Spin-Orbital Coupling in L 1 0 FePdPt Films: Experiments and *Ab Initio* Calculations, *Physical Review Letters* **110**, 10.1103/PhysRevLett.110.077203 (2013).